Current Opinion in Electrochemistry 29 Jan 2019

3D porous metal electrodes: fabrication, characterisation and use

L.F. Arenas,* F.C. Walsh, C. Ponce de León

Electrochemical Engineering Laboratory, Energy Technology Research Group, Faculty of Engineering and Physical Sciences, University of Southampton, Highfield, Southampton, SO17 1BJ, United Kingdom

* Corresponding author: Arenas, Luis Fernando (lfam1c17@soton.ac.uk)

Abstract

Diverse 3D porous metal electrodes, including meshes, foams and felts, are used in electrochemical flow reactors for a wide range of industrial applications, such as energy storage, electrosynthesis and degradation of pollutants. Recent work centres on the hierarchical decoration and coating of 3D electrodes with catalysts, although the study of their performance in a controlled and reproducible flow and mass transfer environment ought to receive more attention. New advances have considered metal nanofelts and nanomesh porous electrodes which show superior productivity. Opportunities are found in additive manufacturing, advanced structural characterization by e.g., X-ray computed tomography, and in 3D modelling of the hydrodynamic characteristics, current distribution and mass transfer coefficient.

Keywords: current distribution, electrochemical flow reactor, felt, foam, porous electrodes, three-dimensional electrodes

(2,670 words, 4 figures)

Introduction

The benefits of conductive 3D, porous materials in electrochemical technology are numerous, particularly in electrochemical flow reactors where process intensification can be realised and scale-up data can be obtained [1]. Compared to 2D structures, porous materials offer a significantly larger surface area; in devices for continuous processing, such as filter press and trickle tower reactors, the electrolyte flow through their structure enhances mass transfer. Reticulated vitreous carbon and carbon felt are often convenient and cost-effective. However, many applications require electrodes with better corrosion resistance, higher electrical conductivity, superior mechanical properties or the possibility of being coated with tailored electrocatalysts. Metal-based porous electrodes accommodate such needs and are found as packed beds, perforated plates, foams, expanded or woven mesh, micromesh, cloths and textile-like, felts, 'paper' and 'wool'. Crucially, functional coatings on such materials are possible. Such diversity offers important possibilities for innovative and tailored solutions in electrochemical engineering.

Porous metal electrodes are often studied in terms of their electrocatalytic properties, particularly the effect of coating or decorating their surface, as well as the coating conditions (e.g. electrodeposition) and ageing mechanisms (e.g. corrosion). Applied electrochemistry often considers these materials as electrodes in static and flow cells used for electrosynthesis, water treatment, destruction of pollutants and environmental remediation, as well as energy conversion and storage. In these cases, space-time yield and energy efficiency are important, and considerations such as current distribution, electrolyte fluid flow, mass transfer, hydraulic permeability (all of which can be modelled) become relevant. A compromise must be found between proposed new

manufacture and surface modification methods and the characterization of performance in the target application. This work considers recent advances and trends in porous metal electrodes as well as research needs for advanced applications and the rigorous characterisation and modelling of such materials. 3D and porous metals in fuel cells with gas reactants, biosensors, supercapacitors and Li-ion batteries are out of the scope of this work.

Manufacturing methods

Metal felts are usually obtained via melt spun and sintered metal processes. The most relevant type is Pt/Ti felt [2],[3], due to its corrosion resistance. Other common felts are Ir/Ti [4], Rh-Ru/Ti [5] and stainless steel (SS) felt [6]. The contact resistance of electrical connections to felts, either by compression or by spot-welding, has been considered [7]. Aiming to increase the productivity of such electrodes, the concept of 'nanofelts' has recently been demonstrated in a soon to be published research (M.J. Kim *et al.*, ChemRxiv doi: 10.26434/chemrxiv.7468703). The flow-through electrode was made with 220 nm diameter Cu nanowires, having a surface area approx. 15 times that of carbon felt and affording the highest reported value of volumetric mass transfer coefficient, with a relationship to mean linear flow rate of $k_m A_e = 36.5v^{0.77}$. In a reductive dehalogenation, the single pass conversion was over 4.2 times that of a carbon felt at a given flow rate, albeit with a higher pressure drop. Microtubular, nanoporous Cu fibres could also be used to make flow electrodes [8].

Common open-foam electrodes (Ni, SS, Ti, Cu, and Al) are generally made via casting, electroless deposition of metal coatings on polyurethane precursors or powder metallurgy

[9]. Recent work has considered lost carbonate sintering for Ni [10], instead of the usual electroless method. All of these techniques result in randomly organised pores. However, advances have been made towards organized foams having specific geometries using selective laser melting of metal powder. These include '3D-printed' SS foam-like porous electrodes for flow cells, such as tailorable Ni-coated [11] or cellular SS electrodes for oxygen evolution [12].

Mechanical tooling and machining methods to make perforated plates or expanded meshes can hardly be improved. Therefore, new advances have been made through different manufacturing techniques. For instance, 3D printed mesh-like SS electrodes with integrated helical mixers [13]. Meanwhile, spiral-wound woven SS mesh has been studied as a substitute to woven mesh [14]. Metal fibre cloths can be contrasted to 'embroidered electrodes' in flexible polymer fabrics [15]. As in the case of felts, novelty has been achieved by producing Ni 'nanomesh' using an aluminium oxide template [16]. As shown in Fig. 1, this material resembles an ordered wire scaffold. Mass transport and pressure drop are yet to be investigated.

Surface modification strategies

A multitude of surface modification strategies can be applied to porous metal electrodes [1]. However, only a fraction of these provide a satisfactory compromise among chemical, electrochemical and mechanical stability, morphology and degree of coverage suitable for technical applications. Electrodeposition is often used to coat materials with catalysts. A classic example is Pt on Ti substrates, such as felt [2],[3] and mesh [17],[18]. Other examples on Ti are Ir [4] and Rh and Ru [5] on felt or Sb on Ti foam [19].

Electrodeposition of Ni is also common, e.g., on Ti foam [20], although it is more often seen as a coating on SS, e.g., in 3D printed electrodes [11]. Ru-polypyrrole [21], pure Pd [22] and NiOOH [23] have been deposited on Ni foam in the same manner. Meanwhile, Cu foam has been electrodeposited with MoS_x [24]. It must be noted that the distribution of electrodeposits is strongly influenced by the current distribution [2],[18]. An alternative electrochemical approach is to 'immersion plate', as to coat SS with Pt [25]. This technique is readily achieved on Ni foam, for Pt [26], Pt-Ru [27], TiC-doped Pd [28], Pd [29] and Ag [30] coatings. Limitations arise due to a restricted thickness and surface porosity of the coatings. Anodized electrocatalysts are also feasible, such as CuO wires [31], along Ti_3C_2-modified Ni foam by electrophoresis [32]. Authors often forget the elegance of monitoring the coating process by measuring the open-circuit potential.

Thermal and annealing methods have produced Cu_2O/TiO_2 on Cu foam [33], Fe-doped $Ni(OH)_2$ on Ni foam by dip-coating [34], carbon on Al foam [35]. Fig. 2 shows hierarchical ZnO nanowires grown on CuO nanowires on Cu foam prepared through a combination of chemical and hydrothermal processes [36]. Such work illustrates well the possibility of modifying macroscopic porous electrodes with nanostructured catalysts. Other techniques involve sputtering of Ir on Ti felt [4], plasma discharge of CuO-NiO nanowires on Ni foam [37] or thermal vapour deposition of $NiSe_2$ on Ni foam [38], freeze-drying of $PdPt_x$ alloy graphene-Ni foam [39] and carbon nanofibers on Ni foam from C_2H_4 [40]. Chemical vapour deposition (CVD) is useful to form carbon coatings, such as amorphous carbon on SS felt [6], N-doped graphene on Cu foam [41] decorated N-doped carbon nanotubes (CNT) on Ni foam [42], or CNT by plasma-enhanced chemical vapour deposition (PECVD) on embroidered Cu wires [43]. Boron-doped diamond (BDD) coatings are applicable to Ti, Nb and Mo porous structures [44].

Much activity has been shown in hydrothermal micro and nanostructured coatings on Ni foam. Examples include WS_2 flakes [45], Pd-SnO_2 nanorods [46], MnO_2 nanospheres [47], $NiCo_2S_4$ networks [48], Co_3O_4 nanowires and nanoflowers [49],[50], $NiCo_2O_4$ [51] and $MoNi_4$ [52] microflowers, and NiO nanowalls [53] plus hierarchical $NiCo_2O_4$ nanowires grown on Ni foam [54]. Enhanced surface area and catalytic activity are achieved but long-term structural stability needs further study.

Advanced imaging characterization

The latest addition to the array of structural and morphological characterization of porous electrodes consist in high-resolution X-ray computed microtomography (CT). Combined with digital image postprocessing, properties such as porosity, tortuosity, surface area and composition can be analysed in detail. Electrochemical surface area can be contrasted to the physical surface area obtained from CT. For instance, Fig. 3 shows the analysis of bare Ti felt by CT, which afforded characteristics such as porosity and volumetric surface area. It must be stressed, however, that the calculated surface area depends on the resolution, thresholding method and processing algorithm [55]. For metals, only the porosity of a 3D printed Ti alloy [56], and the tortuosity of Ni foams [57] have been reported. Composition, quality and uniformity of coating can be assessed as well, as in the case of Pt deposits on Ti felt [2] and micromesh [18] or Ir coating on Ti felt [4]. Porosity is often neglected yet vital for corrosion protection and longevity. Digital CT objects could be used to simulate electrolyte fluid flow and pressure drop [58] in electrochemical flow cells.

Performance characterisation

A description of the technological productivity of metal-based porous electrodes supporting redox reactions requires the analysis of both electrode kinetics and mass transfer conditions. Furthermore, it is generally necessary to incorporate reference electrodes in each half-cell to express cell potential in terms of its thermodynamic, kinetic and ohmic components. Stirred beaker cells are convenient and provide preliminarily information but fluid flow and mass transfer are difficult to reproduce and scale-up. Porous electrodes are much more effective in flow reactors, where fluid velocity can be controlled and measured, then related to mass transfer and pressure drop, as part of a cost - benefit approach. Techniques should be chosen by their speed, convenience and agreement.

Recent examples of controlled electrolyte flow and mass transfer studies are found for various types of Pt and Ir-coated 3D titanium substrates [59],[60], *via* limiting current measurement. Advances could be made by studying the conversion rates and mass transfer coefficient at low Reynolds numbers using simulation or by separating the electrode kinetics from the mass transfer contribution using Koutecky-Levich equation. The maximum electrochemical conversion can be corelated to the experimental, normalised pressure drop across the porous electrodes [61], allowing electrolyte pumping requirements to be calculated and costed. New techniques could simulate permeability and pressure drop from the known digital structure of the foam [58].

Recent and novel applications

Renewed attention to organic electrosynthesis is evident in recent reviews [62]. Many reactions can be carried out advantageously on 3D electrodes. Fewer inorganic synthesis reactions have been considered but important examples are NH_3 synthesis on Rh and Ru/Ti felts [5] or CO_2 reduction at Cu or Ir/Ti felts [63]. Many applications of porous electrodes are related to the degradation of pollutants for environmental remediation and water treatment. The degradation of highly toxic compounds is an important example. Common dichlorination reactions are those of herbicides [30], urea [53], triclosan [41], pentachlorophenol [21] and 2,4-dichlorobenzoic acid [28]. Oxidation of compounds for decontamination is typical, and has been applied to remove benzene at Sb-SnO_2 Ti foam [19]. It is unfortunate that most studies consider only loss of the aqueous contaminant, rather than any intermediates formed (which can be gaseous, toxic or persistent).

Water electrolysis is an important application. For the hydrogen evolution reaction (HER), catalysts such as Pt [26], $MoNi_4$ [52] and $NiCo_2S_4$ [48] can be deposited on Ni foam. Similarly, Cu_2O/TiO_2 [33] or MoS_x [24] on Cu foam. For the oxygen evolution reaction (OER), the latest activity has been dedicated to catalysts on Ni foam, such as WS_2 [45], S-$NiFe_2O$ on Ti_3C_2 [32], and Fe-doped $Ni(OH)_2$ [34]; or on SS, such as $Ni(Fe)O_xH_y$ [64]. Porous electrodes made of SS could be reconsidered [65]. Meanwhile, PEM electrolysis continues using noble metals, such as Ir/Ti felts [4].

Many types of fuel cells with liquid reactants, for instance, ethanol [66], methanol [49], and urea-H_2O_2 [67] types employ porous electrodes. Higher power devices include direct borohydride fuel cells using Pt-Ti felt and micromesh [60], hydrazine using Pd-Ni foam [22], and H_2O_2 using Pd-SnO_2/Ni foam [46]. Of these, only the borohydride type, and

cerium-based redox flow batteries [59], have been studied in terms of electrolyte flow. Static metal air batteries employing Ni foam modified electrodes have also been considered, such as Zn-air [47], [50].

Among the previous publications, scalable studies performed in cells with reproducible mass transfer environment are disappointingly scarce. Most of the claimed applications restrict themselves to short term voltammetric techniques. In a few cases, otherwise valuable contributions have attempted inadequate scale-up, i.e., employing non-reproducible mass transfer environments or not reporting them at all. Realistic figures of merit require attention to the principles of electrochemical engineering and chemical processing [1].

Reproducible, predictable mass transfer rates are better attained by the use of flow-through or flow-by flow cells in batch recirculation. Applications studied in this manner can be found in the field of energy storage, e.g., cerium-based flow batteries [59] or borohydride fuel cells [60], while recent examples on electrochemical processing are the electrodegradation of resorcinol [29], the recycling of Cu(II) etchant [68], and the production of 2,5-furandicarboxylic acid from biomass [23]. Fig. 4 shows the two-cell stack pilot electrochemical flow cell employing Ni foam electrodes. Several examples of porous electrodes in flow cells are found in the field of electrochemical water treatment, e.g., electro-generation of H_2O_2 and electro-Fenton at coated Al foam [35], as well as RuO_2/IrO_2 Ti mesh and thin-film BDD on a Nb mesh electrodes [69]. Other controlled reaction environments are the rotating cylinder electrode and packed bed electrochemical

flow reactors. Recent examples include the removal of Cd in a woven wire rotating mesh [14], and water treatment using a packed bed of iron particles [70].

Mass transfer studies for flow-through foam electrodes have been attempted in beaker cells with a recirculating electrolyte [10] and anodic Fenton oxidations have been studied in aerated batch cells [71]. However, these can be considered only as preliminary steps towards flow cell studies. Appropriate batch studies carried out in stirred beakers can be a useful first step towards scale-up, e.g., electrode the oxidation of ammonia at NiOOH/Ni-foam [72]. Stirred beaker cells offer a very convenient laboratory facility but a poorly-defined reaction environment regarding fluid flow and mass transfer.

Mathematical modelling

Current, potential and concentration distribution models for porous metal electrodes are critical to the simulation of electrochemical operations and to the understanding of their local reaction environment. The classical problem at 3D porous electrodes is the determination of the potential drop and local current density across their thickness and the related optimal thickness and length in flow reactors. Analytical approaches have developed models beyond the usual assumption of low conversion per pass in flow-through electrodes [73],[74], and optimized their thickness under kinetic control conditions [75]. Other recent work has incorporated the potential distribution and the effect of bubbles in flow-across, SS felt electrodes [76]. In contrast to carbon-based materials, multiphysics and 3D models are less common for metal porous electrodes, one example being a fuel cell with an Al foam [77].

Opportunities are found in 3D modelling of metal porous electrodes in electrochemical flow reactors, especially in view of the possibility of capturing their geometry by digital imaging and computation, e.g. via CT [55],[78]. In addition to enabling modelling of current distribution, such methods could model electrolyte flow, pressure drop and mass transport coefficients. For instance, Reynolds average Navier-Stokes (RANS) equations for turbulent flow can be used to describe flow in porous structures [79]. Other types of model, including geometrical and mechanical foams based on Weaire-Phelan structures [80], remain relevant.

Conclusion and outlook

3D porous metal electrodes having superior surface area and enhanced mass transfer coefficients than 2D plates and sheets will continue to be the main choice in productive electrochemical reactors. Numerous manufacture techniques and surface modification strategies are possible. Important recent trends are found in the decoration of open-cell metal foams with hierarchical structures, the implementation of additive manufacturing for niche applications and the development of nanostructured metal felts and meshes. Rigorous studies on electrodeposition on porous electrodes are rare, notwithstanding its importance to applied settings. Many studies claiming industrial applications are limited to voltammetric and batch studies, with insufficient attention to scale-up parameters or controlled mass transfer environment. Awareness of mean linear electrolyte flow rate and mass transport coefficients must spread in this field. Meanwhile, many surface decoration methods report non-uniform deposits, lack durability studies and, in some cases, fail to report basic characteristics, such as volumetric porosity. Future research must consider improvements in these areas. Analytical models of porous electrodes continue to be developed, but new opportunities are found in 3D and multiphysics modelling of current

distribution, fluid flow, mass transfer and reactant conversion over time. CT is incipiently used in metrological analysis of porous structures and in the characterisation of electrodeposited catalysts.

Acknowledgements

LFA and CPL acknowledge the financial support of Newton Fund and Innovate UK. LFA thanks FCW for additional support through RIFI (University of Southampton).

References and recommended reading

Papers of particular interest, published within the period of review, have been highlighted as:

• Paper of special interest

•• Paper of outstanding interest.

[1] F.C. Walsh, L.F. Arenas, C. Ponce de León, Developments in electrode design: structure, decoration and applications of electrodes for electrochemical technology, J. Chem. Technol. Biotechnol. 93 (2018) 3073–3090. doi:10.1002/jctb.5706.

[2] • L.F. Arenas, C. Ponce de León, R.P. Boardman, F.C. Walsh, Electrodeposition of platinum on titanium felt in a rectangular channel flow cell, J. Electrochem. Soc. 164 (2017) D57–D66. doi:10.1149/2.0651702jes.

Demonstrates the effect of current distribution on electrodeposition on porous metal electrodes as studied by X-ray computed tomography.

[3] U. Rost, P. Podleschny, M. Schumacher, R. Muntean, D.T. Pascal, C. Mutascu, et al., Long-term stable electrodes based on platinum electrocatalysts supported on titanium sintered felt for the use in PEM fuel cells, IOP Conf. Ser.: Mater. Sci. Eng. 416 (2018) 012013. doi:10.1088/1757-899X/416/1/012013.

[4] C. Liu, M. Carmo, G. Bender, A. Everwand, T. Lickert, J.L. Young, et al., Performance enhancement of PEM electrolyzers through iridium-coated

titanium porous transport layers, Electrochem. Commun. 97 (2018) 96–99. doi:10.1016/j.elecom.2018.10.021.

[5] K. Kugler, M. Luhn, J.A. Schramm, K. Rahimi, M. Wessling, Galvanic deposition of Rh and Ru on randomly structured Ti felts for the electrochemical NH_3 synthesis, Phys. Chem. Chem. Phys. 17 (2015) 3768–3782. doi:10.1039/C4CP05501B.

[6] H. Feng, C. Tang, Q. Wang, Y. Liang, D. Shen, K. Guo, et al., A novel photoactive and three-dimensional stainless steel anode dramatically enhances the current density of bioelectrochemical systems, Chemosphere. 196 (2018) 476–481. doi:10.1016/j.chemosphere.2017.12.166.

[7] M.-N. Feng, Y. Xie, C.-F. Zhao, Z. Luo, Microstructure and mechanical performance of ultrasonic spot welded open-cell Cu foam/Al joint, Journal of Manufacturing Processes. 33 (2018) 86–95.

[8] R. Kas, K.K. Hummadi, R. Kortlever, P. de Wit, A. Milbrat, M.W.J. Luiten-Olieman, et al., Three-dimensional porous hollow fibre copper electrodes for efficient and high-rate electrochemical carbon dioxide reduction, Nature Communications. 7 (2016) 364. doi:10.1038/ncomms10748.

[9] F. García-Moreno, Commercial applications of metal foams: Their properties and production, Materials 2016, Vol. 9, Page 85. 9 (2016) 85. doi:10.3390/ma9020085.

[10] P. Zhu, Y. Zhao, Mass transfer performance of porous nickel manufactured by lost carbonate sintering process, Advanced Engineering Materials. 162 (2017) 1700392–8. doi:10.1002/adem.201700392.

[11] •• L.F. Arenas, C. Ponce de León, F.C. Walsh, 3D-printed porous electrodes for advanced electrochemical flow reactors: A Ni/stainless steel electrode and its mass transport characteristics, Electrochem. Commun. 77 (2017) 133–137.

Introduces the concept of additive manufacturing for tailored porous electrodes.

[12] X. Huang, S. Chang, W.S.V. Lee, J. Ding, J.M. Xue, Three-dimensional printed cellular stainless steel as a high-activity catalytic electrode for oxygen evolution, J. Mater. Chem. A. 5 (2017) 18176–18182. doi:10.1039/C7TA03023A.

[13] J. Lölsberg, O. Starck, S. Stiefel, J. Hereijgers, T. Breugelmans, M. Wessling, 3D-printed electrodes with improved mass transport properties, ChemElectroChem. (2017). doi:10.1002/celc.201700662.

[14] A.H. Abbar, R.H. Salman, A.S. Abbas, Cadmium removal using a spiral-wound woven wire meshes packed bed rotating cylinder electrode, Environmental Technology & Innovation. (2018). doi:10.1016/j.eti.2018.12.005.

[15] N. Aguiló-Aguayo, T. Bechtold, Monitoring the state-of-charge in all-iron aqueous redox flow batteries, J. Electrochem. Soc. 165 (2018) A3164–A3168.

[16] •• S.P. Zankowski, P.M. Vereecken, Combining high porosity with high surface area in flexible interconnected nanowire meshes for hydrogen generation and beyond, ACS Appl. Mater. Interfaces. 10 (2018) 44634–44644. doi:10.1021/acsami.8b15888.

Presents a highly structured, mesh-like porous metal electrode produced by a template method.

[17] U.M. López-García, P.E. Hidalgo, J.C. Olvera, F. Castañeda, H. Ruiz, G. Orozco, The hydrodynamic behavior of a parallel-plate electrochemical reactor, Fuel. 110 (2013) 162–170. doi:10.1016/j.fuel.2012.11.016.

[18] L.F. Arenas, C. Ponce de León, R.P. Boardman, F.C. Walsh, Characterisation of platinum electrodeposits on a titanium micromesh stack in a rectangular channel flow cell, Electrochim. Acta. 247 (2017) 994–1005. doi:10.1016/j.electacta.2017.07.029.

[19] B. Zhang, M. Chen, C. Zhang, H. He, Electrochemical oxidation of gaseous benzene on a Sb-SnO2/foam Ti nano-coating electrode in all-solid cell, Chemosphere. 217 (2019) 780–789. doi:10.1016/j.chemosphere.2018.10.222.

[20] I. Satar, W.R.W. Daud, B.H. Kim, M.R. Somalu, M. Ghasemi, M.H.A. Bakar, et al., Performance of titanium–nickel (Ti/Ni) and graphite felt-nickel (GF/Ni) electrodeposited by Ni as alternative cathodes for microbial fuel cells, J. Taiwan Inst. Chem. Eng. 89 (2018) 67–76. doi:10.1016/j.jtice.2018.04.010.

[21] J. Wang, C. Cui, Y. Xin, Q. Zheng, X. Zhang, High-performance electrocatalytic hydrodechlorination of pentachlorophenol by amorphous Ru-loaded polypyrrole/foam nickel electrode, Electrochim. Acta. 296 (2019) 874–881. doi:10.1016/j.electacta.2018.11.115.

[22] L.-S. Wu, X.-P. Wen, H. Wen, H.-B. Dai, P. Wang, Palladium decorated porous nickel having enhanced electrocatalytic performance for hydrazine oxidation, J. Power Sources. 412 (2019) 71–77. doi:10.1016/j.jpowsour.2018.11.023.

[23] •• R. Latsuzbaia, R. Bisselink, A. Anastasopol, H. van der Meer, R. van Heck, M.S. Yagüe, et al., Continuous electrochemical oxidation of biomass derived 5-(hydroxymethyl)furfural into 2,5-furandicarboxylic acid, J. Appl. Electrochem. 48 (2018) 611–626. doi:10.1007/s10800-018-1157-7.

Presents a recent pilot-scale industrial process showcasing the advantages and relevance of 3D metal electrodes.

[24] S. Min, J. Qin, W. Hai, Y. Lei, J. Hou, F. Wang, Electrochemical growth of MoSx on Cu foam: A highly active and robust three-dimensional cathode for hydrogen evolution, Int. J. Hydrogen Energy. 43 (2018) 4978–4986. doi:10.1016/j.ijhydene.2018.01.145.

[25] J. Weber, A.J. Wain, H. Piili, V.P. Matilainen, A. Vuorema, G.A. Attard, et al., Residual porosity of 3D-LAM-printed stainless-steel electrodes allows galvanic exchange platinisation, ChemElectroChem. 3 (2016) 1020–1025. doi:10.1002/celc.201600098.

[26] • R.G. Milazzo, S.M.S. Privitera, D. D'Angelo, S. Scalese, S. Di Franco, F. Maita, et al., Spontaneous galvanic displacement of Pt nanostructures on nickel foam: Synthesis, characterization and use for hydrogen evolution reaction, Int. J. Hydrogen Energy. 43 (2018) 7903–7910. doi:10.1016/j.ijhydene.2018.03.042.

A recent example of facile production of highly catalytic platinized-nickel electrodes using galvanic displacement.

[27] H. Wang, H. Yu, S. Yin, Y. Xu, X. Li, Y. Yamauchi, et al., In situ coating of a continuous mesoporous bimetallic PtRu film on Ni foam: a nanoarchitectured self-standing all-metal mesoporous electrode, J. Mater. Chem. A. 6 (2018) 12744–12750. doi:10.1039/C8TA03413C.

[28] Z. Lou, Y. Li, J. Zhou, K. Yang, Y. Liu, S.A. Baig, et al., TiC doped palladium/nickel foam cathode for electrocatalytic hydrodechlorination of 2,4-DCBA: Enhanced electrical conductivity and reactive activity, J. Hazard. Mater. 362 (2019) 148–159. doi:10.1016/j.jhazmat.2018.08.066.

[29] T. Mikolajczyk, B. Pierozynski, L. Smoczynski, W. Wiczkowski, Electrodegradation of resorcinol on pure and catalyst-modified Ni foam anodes, studied under alkaline and neutral pH conditions, Molecules. 23 (2018) 1293. doi:10.3390/molecules23061293.

[30] E. Verlato, W. He, A. Amrane, S. Barison, D. Floner, F. Fourcade, et al., Preparation of silver-modified nickel foams by galvanic displacement and their use as cathodes for the reductive dechlorination of herbicides, ChemElectroChem. 3 (2016) 2084–2092. doi:10.1002/celc.201600214.

[31] Z. Li, Y. Chen, Y. Xin, Z. Zhang, Sensitive electrochemical nonenzymatic glucose sensing based on anodized CuO nanowires on three-dimensional porous copper foam, Sci. Rep. 5 (2015) 16115. doi:10.1038/srep16115.

[32] Y. Tang, C. Yang, Y. Yang, X. Yin, W. Que, J. Zhu, Three dimensional hierarchical network structure of S-$NiFe_2O_4$ modified few-layer titanium carbides (MXene) flakes on nickel foam as a high efficient electrocatalyst for oxygen evolution, Electrochim. Acta. 296 (2019) 762–770. doi:10.1016/j.electacta.2018.11.083.

[33] B. Long, H. Yang, M. Li, M.-S. Balogun, W. Mai, G. Ouyang, et al., Interface charges redistribution enhanced monolithic etched copper foam-based Cu_2O layer/TiO_2 nanodots heterojunction with high hydrogen evolution electrocatalytic activity, Applied Catalysis B: Environmental. 243 (2019) 365–372. doi:10.1016/j.apcatb.2018.10.039.

[34] C.X. Guo, C.M. Li, Room temperature-formed iron-doped nickel hydroxide on nickel foam as a 3D electrode for low polarized and high-current-density oxygen evolution, Chem. Commun. 54 (2018) 3262–3265. doi:10.1039/C8CC00701B.

[35] J.F. Pérez, J. Llanos, C. Sáez, C. López, P. Cañizares, M.A. Rodrigo, Towards the scale up of a pressurized-jet microfluidic flow-through reactor for cost-effective electro-generation of H_2O_2, J. Clean. Prod. 211 (2019) 1259–1267. doi:10.1016/j.jclepro.2018.11.225.

[36] • C. Wang, L. Yue, S. Wang, Y. Pu, X. Zhang, X. Hao, et al., Role of electric field and reactive oxygen species in enhancing antibacterial activity: a case study of 3D Cu foam electrode with branched CuO–ZnO NWs, J. Phys. Chem. C. 122 (2018) 26454–26463. doi:10.1021/acs.jpcc.8b08232.

An example of a doubly hierarchical porous metal electrode comprising of ZnO nanowires grown on CuO nanowires on a nickel foam.

[37] C. Li, B. Zhang, Y. Li, S. Hao, X. Cao, G. Yang, et al., Self-assembled Cu-Ni bimetal oxide 3D in-plane epitaxial structures for highly efficient oxygen evolution reaction, Applied Catalysis B: Environmental. 244 (2019) 56–62. doi:10.1016/j.apcatb.2018.11.046.

[38] H. Zhou, Y. Wang, R. He, F. Yu, J. Sun, F. Wang, et al., One-step synthesis of self-supported porous $NiSe_2$/Ni hybrid foam: An efficient 3D electrode for hydrogen evolution reaction, Nano Energy. 20 (2016) 29–36. doi:10.1016/j.nanoen.2015.12.008.

[39] C.H.A. Tsang, K.N. Hui, K.S. Hui, Influence of Pd_1Pt_x alloy NPs on graphene aerogel/nickel foam as binder-free anodic electrode for electrocatalytic ethanol oxidation reaction, J. Power Sources. 413 (2019) 98–106. doi:10.1016/j.jpowsour.2018.12.019.

[40] J.M.R. van Beek, Z.J. Wang, A. Rinaldi, M.G. Willinger, L. Lefferts, Initiation of carbon nanofiber growth on polycrystalline nickel foam under low ethylene pressure, ChemCatChem. 10 (2018) 3107–3114. doi:10.1002/cctc.201701838.

[41] R. Mao, C. Huang, X. Zhao, M. Ma, J. Qu, Dechlorination of triclosan by enhanced atomic hydrogen-mediated electrochemical reduction: Kinetics, mechanism, and toxicity assessment, Applied Catalysis B: Environmental. 241 (2019) 120–129. doi:10.1016/j.apcatb.2018.09.013.

[42] H. Zhang, L. Zhang, Y. Han, Y. Yu, M. Xu, X. Zhang, et al., RGO/Au NPs/N-doped CNTs supported on nickel foam as an anode for enzymatic biofuel cells, Biosensors and Bioelectronic. 97 (2017) 34–40. doi:10.1016/j.bios.2017.05.030.

[43] • N. Aguiló-Aguayo, R. Amade, S. Hussain, E. Bertran, T. Bechtold, New three-dimensional porous electrode concept: vertically-aligned carbon nanotubes

directly grown on embroidered copper structures, Nanomaterials. 7 (2017) 438. doi:10.3390/nano7120438.

Presents the concept of embroidered wire electrodes as an alternative to woven meshes.

[44] Y. He, H. Lin, Z. Guo, W. Zhang, H. Li, W. Huang, Recent developments and advances in boron-doped diamond electrodes for electrochemical oxidation of organic pollutants, Sep Pur Technol. 212 (2019) 802–821. doi:10.1016/j.seppur.2018.11.056.

[45] K. Hu, J. Zhou, Z. Yi, C. Ye, H. Dong, K. Yan, Facile synthesis of mesoporous WS2 for water oxidation, Applied Surface Science. 465 (2019) 351–356. doi:10.1016/j.apsusc.2018.09.179.

[46] L. Sun, W. He, S. Li, L. Shi, Y. Zhang, J. Liu, The high performance mushroom-like Pd@SnO2/Ni foam electrode for H2O2 reduction in alkaline media, J. Power Sources. 395 (2018) 386–394. doi:10.1016/j.jpowsour.2018.05.056.

[47] K. Xu, A. Loh, B. Wang, X. Li, Enhancement of oxygen transfer by design nickel foam electrode for zinc−air battery, J. Electrochem. Soc. 165 (2018) A809–A818. doi:10.1149/2.0361805jes.

[48] H. Liu, X. Ma, Y. Rao, Y. Liu, J. Liu, L. Wang, et al., Heteromorphic $NiCo_2S_4/Ni_3S_2$/Ni Foam as a self-standing electrode for hydrogen evolution reaction in alkaline solution, ACS Appl. Mater. Interfaces. 10 (2018) 10890–10897. doi:10.1021/acsami.8b00296.

[49] G. Rajeshkhanna, G. Ranga Rao, Micro and nano-architectures of Co_3O_4 on Ni foam for electro-oxidation of methanol, Int. J. Hydrogen Energy. 43 (2018) 4706–4715. doi:10.1016/j.ijhydene.2017.10.110.

[50] P. Tan, B. Chen, H. Xu, W. Cai, W. He, M. Ni, In-situ growth of Co_3O_4 nanowire-assembled clusters on nickel foam for aqueous rechargeable Zn-Co3O4 and Zn-air batteries, Applied Catalysis B: Environmental. 241 (2019) 104–112. doi:10.1016/j.apcatb.2018.09.017.

[51] Y. Wang, D. Liu, K. Cao, In situ construction of porous $NiCo_2O_4$/Ni foam electrodes for high-performance energy storage applications, J Porous Mater. 25 (2017) 565–570. doi:10.1007/s10934-017-0469-z.

[52] Y. Jin, X. Yue, C. Shu, S. Huang, P.K. Shen, Three-dimensional porous $MoNi_4$ networks constructed by nanosheets as bifunctional electrocatalysts for overall water splitting, J. Mater. Chem. A. 5 (2017) 2508–2513. doi:10.1039/C6TA10802D.

[53] S. Zhan, Z. Zhou, M. Liu, Y. Jiao, H. Wang, 3D NiO nanowalls grown on Ni foam for highly efficient electro-oxidation of urea, Catalysis Today. (2018). doi:10.1016/j.cattod.2018.02.049.

[54] • L. Sha, K. Ye, G. Wang, J. Shao, K. Zhu, K. Cheng, et al., Hierarchical $NiCo_2O_4$ nanowire array supported on Ni foam for efficient urea electrooxidation in alkaline medium, J. Power Sources. 412 (2019) 265–271. doi:10.1016/j.jpowsour.2018.11.059.

An example of controlled nanowire assembly on nickel foam, resulting in a hierarchical electrode.

[55] L.F. Arenas, R.P. Boardman, C. Ponce de León, F.C. Walsh, X-ray computed micro-tomography of reticulated vitreous carbon, Carbon. 135 (2018) 85–94. doi:10.1016/j.carbon.2018.03.088.

[56] F. Zanini, S. Carmignato, E. Savio, Enhancing CT porosity measurements on metal additive manufactured parts, (2017).

[57] B. Tjaden, D.J.L. Brett, P.R. Shearing, Tortuosity in electrochemical devices: a review of calculation approaches, Int. Mater. Rev. 63 (2016) 47–67. doi:10.1080/09506608.2016.1249995.

[58] X. Ou, X. Zhang, T. Lowe, R. Blanc, M.N. Rad, Y. Wang, et al., X-ray micro computed tomography characterization of cellular SiC foams for their applications in chemical engineering, Mater. Charact. 123 (2017) 20–28. doi:10.1016/j.matchar.2016.11.013.

[59] L.F. Arenas, C. Ponce de León, F.C. Walsh, Mass transport and active area of porous Pt/Ti electrodes for the Zn-Ce redox flow battery determined from limiting current measurements, Electrochim. Acta. 221 (2016) 154–166. doi:10.1016/j.electacta.2016.10.097.

[60] •• A.A. Abahussain, C. Ponce de León, F.C. Walsh, Mass-transfer measurements at porous 3D Pt-Ir/Ti electrodes in a direct borohydride fuel cell, J. Electrochem. Soc. 165 (2018) F198–F206. doi:10.1149/2.0751803jes.

Recent flow cell studies at various porous metal electrodes, highlighting the importance of normalized flow rate and mass transfer parameters.

[61] • L.F. Arenas, C. Ponce de León, F.C. Walsh, Pressure drop through platinized titanium porous electrodes for cerium-based redox flow batteries, AIChE J. 64 (2018) 1135–1146. doi:10.1002/aic.16000.

Demonstrates the correlation of electrochemical performance and hydraulic pressure drop in porous electrodes needed for cell and reactor design.

[62] D. Pletcher, R.A. Green, R.C.D. Brown, Flow electrolysis cells for the synthetic organic chemistry laboratory, Chem. Rev. 118 (2017) 4573–4591. doi:10.1021/acs.chemrev.7b00360.

[63] S.M.A. Kriescher, K. Kugler, S.S. Hosseiny, Y. Gendel, M. Wessling, A membrane electrode assembly for the electrochemical synthesis of

hydrocarbons from CO_2(g) and H_2O(g), Electrochem. Commun. 50 (2015) 64–68. doi:10.1016/j.elecom.2014.11.014.

[64] Q. Zhang, H. Zhong, F. Meng, D. Bao, X. Zhang, X. Wei, Three-dimensional interconnected Ni(Fe)OxHy nanosheets on stainless steel mesh as a robust integrated oxygen evolution electrode, Nano Res. 11 (2018) 1294–1300. doi:10.1007/s12274-017-1743-8.

[65] H. Schäfer, M. Chatenet, Steel: The resurrection of a forgotten water-splitting catalyst, ACS Energy Lett. 3 (2018) 574–591. doi:10.1021/acsenergylett.8b00024.

[66] K.-B. Ma, S.-B. Han, S.-H. Kwon, D.-H. Kwak, K.-W. Park, High-performance direct ethanol fuel cell using nitrate reduction reaction, Int. J. Hydrogen Energy. 43 (2018) 17265–17270. doi:10.1016/j.ijhydene.2018.07.094.

[67] F. Guo, D. Cao, M. Du, K. Ye, G. Wang, W. Zhang, et al., Enhancement of direct urea-hydrogen peroxide fuel cell performance by three-dimensional porous nickel-cobalt anode, J. Power Sources. 307 (2016) 697–704. doi:10.1016/j.jpowsour.2016.01.042.

[68] Y. Chang, L. Deng, X. Meng, W. Zhang, C. Wang, Y. Wang, et al., Closed-loop electrochemical recycling of spent copper(II) from etchant wastewater using a carbon nanotube modified graphite felt anode, Environ. Sci. Technol. 52 (2018) 5940–5948. doi:10.1021/acs.est.7b06298.

[69] • J.F. Pérez, J. Llanos, C. Sáez, C. López, P. Cañizares, M.A. Rodrigo, On the design of a jet-aerated microfluidic flow-through reactor for wastewater treatment by electro-Fenton, Sep. Pur. Technol. 208 (2019) 123–129. doi:10.1016/j.seppur.2018.04.021.

A flow reactor using Al foam electrodes in combination with aeration to enhance the homogeneous oxidation of pollutants.

[70] J. Llanos, J. Isidro, C. Sáez, P. Cañizares, M.A. Rodrigo, Development of a novel electrochemical coagulant dosing unit for water treatment, J. Chem. Technol. Biotechnol. 94 (2019) 216–221. doi:10.1002/jctb.5767.

[71] Y. Zhu, S. Qiu, F. Deng, F. Ma, G. Li, Y. Zheng, Three-dimensional nickel foam electrode for efficient electro-Fenton in a novel reactor, Environ Technol. 27 (2018) 1–11. doi:10.1080/09593330.2018.1509890.

[72] Y.-J. Shih, Y.-H. Huang, C.P. Huang, In-situ electrochemical formation of nickel oxyhydroxide (NiOOH) on metallic nickel foam electrode for the direct oxidation of ammonia in aqueous solution, Electrochim. Acta. 281 (2018) 410–419. doi:10.1016/j.electacta.2018.05.169.

[73] A.I. Maslii, N.P. Poddubnyi, A.Z. Medvedev, Distribution of geometrical current density inside a flow-by porous electrode: Effect of electrode

parameters and electrochemical reactions, Russ. J. Electrochem. 52 (2016) 576–583.

[74] A.I. Masliy, N.P. Poddubny, A.Z. Medvedev, V.O. Lukyanov, Analysis of the distribution of geometrical current density along the direction of solution flow inside flow-by porous electrodes, J. Electroanal. Chem. 757 (2015) 128–136.

[75] • J.W. Haverkort, A theoretical analysis of the optimal electrode thickness and porosity, Electrochim. Acta. 295 (2019) 846–860. doi:10.1016/j.electacta.2018.10.065.

A recent analytical model for current distribution and electrode thickness. Further work could consider the importance of mass transfer.

[76] R. Constanzo, A. Pagliero, J. Quinteros, Bubble formation effect over the potential and current during functioning of 316 L stainless steel porous electrode in a parallel volumetric cell, Canadian Metallurgical Quarterly. 57 (2018) 481–492. doi:10.1080/00084433.2018.1495916.

[77] J.G. Carton, A.G. Olabi, Three-dimensional proton exchange membrane fuel cell model: Comparison of double channel and open pore cellular foam flow plates, Energy. 136 (2017) 185–195. doi:10.1016/j.energy.2016.02.010.

[78] M.D.R. Kok, R. Jervis, T.G. Tranter, M.A. Sadeghi, D.J.L. Brett, P.R. Shearing, et al., Mass transfer in fibrous media with varying anisotropy for flow battery electrodes: Direct numerical simulations with 3D X-ray computed tomography, Chem. Eng. Sci. (2018). doi:10.1016/j.ces.2018.10.049.

[79] • L. Castañeda, R. Antaño, F.F. Rivera, J.L. Nava, Computational fluid dynamic simulations of single-phase flow in a spacer-filled channel of a filter-press electrolyzer, Int. J. Electrochem. Sci. 12 (2017) 7351–7364. doi:10.20964/2017.08.09.

CFD simulations of flow for porous structures, which could be translated to porous metal electrodes.

[80] B. Buffel, F. Desplentere, K. Bracke, I. Verpoest, Modelling open cell-foams based on the Weaire–Phelan unit cell with a minimal surface energy approach, Int. J. Solids Struct. 51 (2014) 3461–3470. doi:10.1016/j.ijsolstr.2014.06.017.

Figure Captions

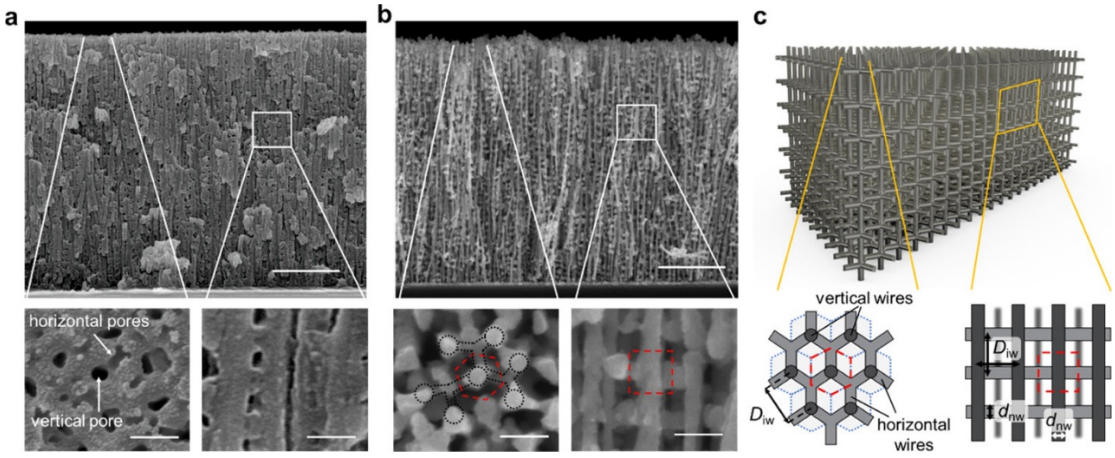

Fig. 1. a) Cross-sectional SEM image of a 3D porous anodic aluminum oxide template, b) Cross-sectional SEM image of the resulting nickel nanomesh, c) Stuctural representation of the porous scafold after template removal, showing its average unit cell. Scale bars: low magnification 1 μm, high magnification 100 nm. Reprinted with permission from Zankowski *et al.* [16], Combining high porosity with high surface area in flexible interconnected nanowire meshes for hydrogen generation and beyond, ACS Applied Materials & Interfaces 10: 44634–44. Copyright (2018) American Chemical Society.

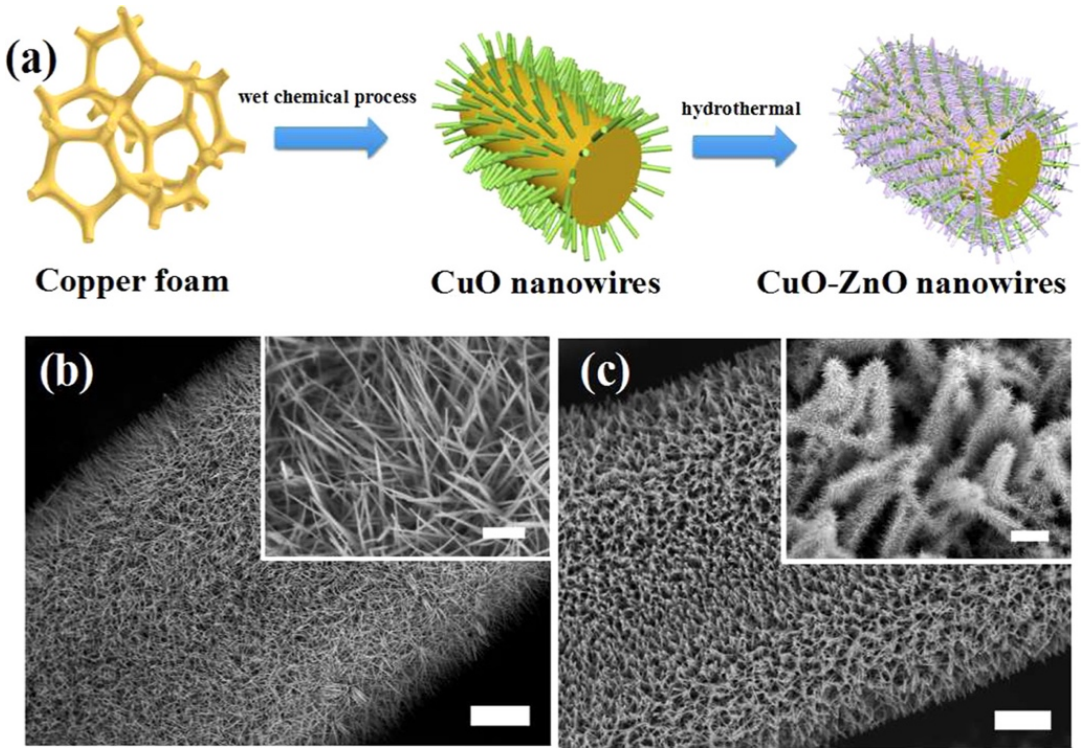

Fig. 2. a) Process for the production of hierarchical CuO-ZnO nanowires on copper foam, b) SEM image of CuO nanowires on a Cu foam strut, and c) of ZnO nanowires branching from the CuO structures. Scale bars: low magnification 10 μm, high magnification 2 μm. Reprinted with permission from Wang *et al.* [36], Role of electric field and reactive oxygen species in enhancing antibacterial activity: a case study of 3D Cu foam electrode with branched CuO–ZnO NWs, The Journal of Physical Chemistry C 122(46): 26454–63. Copyright (2018) American Chemical Society.

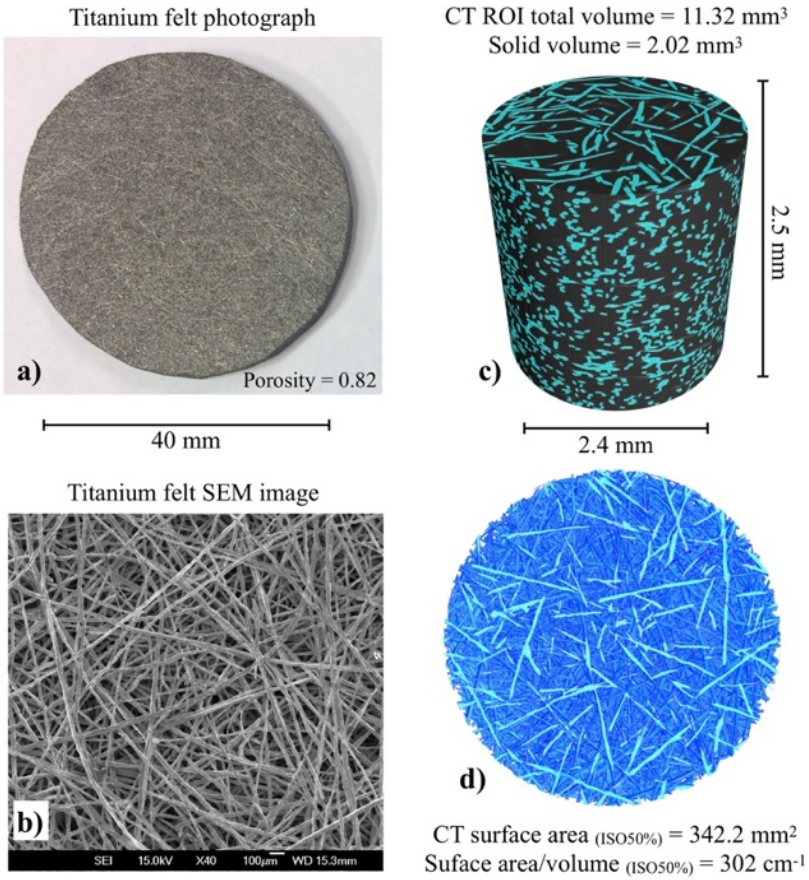

Fig. 3. Structural analysis of titanium felt through CT. a) Bare electrode sample, b) SEM image of titanium fibres, c) cylindrical digital region of interest (ROI) from a scanned sample of felt, d) top-view of a CT binarized image of the fibres. The reported values correspond to a 'ISO50%' thresholding method using VG Studio MAX version 2.1.

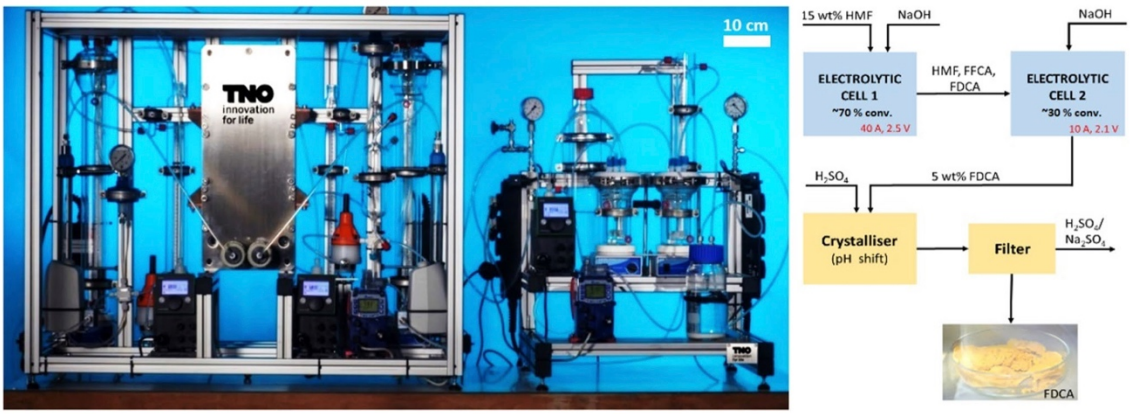

Fig. 4. Bench scale electrochemical flow reactor fitted with two Ni/NiOOH foam (30 ppi or 50 ppi) anodes with projected areas of 400 cm^2 for the two-step production of 2,5-furandicarboxylic acid. Cathodes are stainless steel plates. Reprinted with permission from Latsuzbaia *et al.* [23], Continuous electrochemical oxidation of biomass derived 5-(hydroxymethyl)furfural into 2,5-furandicarboxylic acid, Journal of Applied Electrochemistry 48(6): 611–26. Copyright (2018) Springer Nature.